Multicomponent AM-FM Signals Analysis Based on EMD-B-Splines ESA

Abdelkhalek BOUCHIKHI[1,2] and Abdel-Ouahab BOUDRAA[1]

[1] *IRENav, Ecole Navale, BCRM Brest, CC 600, 29240 Brest Cedex 9, France.*
[2] *RESO, ENIB, Technople Brest-Iroise, CS 73862 - 29238 Brest cedex 3, France.*

Abstract

In this paper a signal analysis framework for estimating time-varying amplitude and frequency functions of multicomponent amplitude and frequency modulated (AM-FM) signals is introduced. This framework is based on local and nonlinear approaches, namely Energy Separation Algorithm (ESA) and Empirical Mode Decomposition (EMD). Conjunction of Discrete ESA (DESA) and EMD is called EMD-DESA. A new modified version of EMD where smoothing instead of an interpolation to construct the upper and lower envelopes of the signal is introduced. Since extracted IMFs are represented in terms of B-spline (BS) expansions, a closed formula of ESA robust against noise is used. Instantaneous Frequency (IF) and Instantaneous Amplitude (IA) estimates of a multicomponent AM-FM signal, corrupted with additive white Gaussian noise of varying SNRs, are analyzed and results compared to ESA, DESA and Hilbert transform-based algorithms. SNR and MSE are used as figures of merit. Regularized BS version of EMD-ESA performs reasonably better in separating IA and IF components compared

Email address: bouchikhi@enib.fr, boudra@ecole-navale.fr (Abdelkhalek BOUCHIKHI[1,2] and Abdel-Ouahab BOUDRAA[1])

Preliminary results of this work has been presented at IEEE ISCCSP, Malta, 2008.

to the other methods from low to high SNR. Overall, obtained results illustrate the effectiveness of the proposed approach in terms of accuracy and robustness against noise to track IF and IA features of a multicomponent AM-FM signal.

Key words: Empirical mode decomposition, Teager-Kaiser operator, Energy separation algorithm, Hilbert transform, AM-FM modeling.

---

1. Introduction

Estimating time-varying amplitude and frequency functions of a multicomponent amplitude and frequency modulated (AM-FM) signal is an area of active interest in signal processing domain. The aim is to understand and describe situations where the frequency content of a signal varies in time (non-stationary signal). In different areas such as in seismic, Radar or Sonar, signals under consideration are known to be non-stationary. Important features of such signals are derived from Instantaneous Frequency (IF) which provides a qualitative information and Instantaneous Amplitude (IA) which gives a quantitative information [1]. Estimating IF and IA functions of analyzed signal is a first step for signals analysis. More specifically, IF determines what frequencies are present, how strong they are, and how they change over time. However, only meaningful IFs could really help one to explain the production, variation and evolution of physical phenomena. The problem of meaningfully interpreting the IF's signal has been addressed in the literature [1]-[3]. It has been argued that the interpretation of IF may be physically appropriate only for monocomponent signals where there is only one spectral component or narrow range of frequencies [1],[3]. Additionally, to reveal true physical meaning of the IF, its estimation must be robust against noise. Though Hilbert Transform (HT) [1] and Energy

Separation Algorithm (ESA) [8], based on Teager-Kaiser Energy Operator (TKEO), are accepted demodulation methods, when applied to multicomponent signal the tracked IF and IA features lose their physical meanings [3]. To overcome this problem, Empirical Mode Decomposition (EMD) was developed so that a multicomponent signal can be analyzed in physically meaningful time-frequency-amplitude space by reducing it to a collection of monocomponent functions [2]. The EMD breaks down any signal into a reduced number of oscillatory modes called Intrinsics Modes Functions (IMFs) such that meaningful IFs and IAs are derived. Many works have been shown that such decomposition can break out physical features [2]-[3],[4]. IMFs extraction is followed by spectral analysis of each mode. Based on EMD two spectral analysis are introduced [2],[6]. Applying HT or Discrete ESA (DESA) to each IMF the derived time-frequency analysis is designated as EMD-HT [2] or EMD-DESA [6]. We have shown that EMD-DESA gives interesting results compared to EMD-HT and particularly for signals with sharp transitions [6]. EMD-DESA works well in moderate noisy environment, but as EMD-HT it performs poorly for very noisy signals. Actually, EMD-DESA limitation is due to the sensitivity to noise of TKEO which is based on signal differentiation. Thus, to reduce noise sensitivity a systematic approach is to use continuous-time expansions of discrete-time signals to numerically implement required differentiations without approximation. Since IMFs are represented in B-spline (BS) expansions [2], a close formulae of TKEO which ensure robustness to noise is used. Also, using a regularized version of BS for interpolation (smoothing) in EMD process, more robustness and better estimates of IF and IA compared to exact version of BS are obtained. Contributions of this paper are as follows:

- Coupling two local and nonlinear approaches (EMD-ESA) as the basis

of a multicomponent AM-FM signal analysis framework. Both IF and IA of a three-component AM-FM signal with varying SNR values are estimated and the associated errors analyzed. The proposed approach is not constrained by the assumptions of stationarity and linearity.

- Compared to Gabor-ESA approach [7] where filterbank of Gabor filters is determined by a set of parameters, the proposed EMD-ESA requires only one input parameter (SD value). Indeed, each Gabor filter requires two parameters: the central filter frequency and the rms bandwidth. Thus, to analyze a signal of K components the Gabor-ESA requires (2K+1) parameters. While in Gabor-ESA K is known, in EMD-ESA this value is determined automatically. Thus, compared to Gabor-ESA, EMD-ESA is a data driven approach.
- Introduction of a new sifting where smoothing instead of interpolation is used to construct the upper and lower envelopes of the signal to be decomposed. Our approach can be easily extended to incorporate other types of splines or smoothing funcions. Advantage of this sifting is to give EMD more robustness against noise and to reduce the number of unwanted IMFs of conventional EMD. The new sifting is analyzed in free and in noisy environment and on a real signal.

2. EMD

EMD aims to analyze a multicomponent signal, $s(t)$, by breaking it down into a finite set of AM-FM zero-mean signals (IMFs) through an iterative process called *sifting* [2]. The decomposition is based on the local time scale of $s(t)$ and yields adaptive basis functions. Locally, each IMF contains lower frequency oscillations, than the just extracted one. EMD does not use predetermined filter and is a fully data driven method [2]. To be successfully

decomposed into IMFs, $s(t)$ must have at least two extrema, one minimum and one maximum. The sifting is shown in table 1, where N denotes the number of IMFs and $\mathrm{r}_N(t)$ is the residual. To guarantee that IMFs retain enough physical sense of both amplitude and frequency modulations, a Standard Deviation (SD) value (Step f) is determined. This is accomplished by limiting the size of SD to ϵ, computed from two consecutive sifting results. Usually, ϵ is set in $[0.2, 0.3]$ [2]. The sifting involves the following steps:

Step 1) Fix ϵ, $j \leftarrow 1$ (j^{th} IMF)

Step 2) $r_{j-1}(t) \leftarrow s(t)$ (residual)

Step 3) Extract the $j-th$ IMF:

- `(a)` $h_{j,i-1}(t) \leftarrow r_{j-1}(t), i \leftarrow 1$ (i number of sifts)
- `(b)` Extract local maxima/minima of $h_{j,i-1}(t)$
- `(c)` Compute upper envelope and lower envelope functions $U_{j,i-1}(t)$ and $L_{j,i-1}(t)$ `by interpolating respectively local maxima and minima of` $h_{j,i-1}(t)$
- `(d)` Compute the envelopes mean: $\mu_{j,i-1}(t) \leftarrow (U_{j,i-1}(t) + L_{j,i-1}(t))/2$
- `(e)` Update: $h_{j,i}(t) \leftarrow h_{j,i-1}(t) - \mu_{j,i-1}(t), i \leftarrow i+1$
- `(f)` Calculate stopping criterion: $SD(i) = \sum_{t=0}^{T} \mid h_{j,i-1}(t) - h_{j,i}(t) \mid^2 / (h_{j,i-1}(t))^2$
- `(g)` Decision: Repeat Step (b)-(f) until $SD(i) < \epsilon$ and then $IMF_j(t) \leftarrow h_{j,i}(t)$

Step 4) Update residual: $r_j(t) \leftarrow r_{j-1}(t) - IMF_j(t)$

Step 5) Repeat Step 3 with $j \leftarrow j+1$ until the number of extrema in $r_j(t) \leq 2$

Table 1: Sifting process

Finally, at the end of the sifting, $s(t)$ is represented as follows :

$$s(t) = \sum_{j=1}^{N} \mathrm{IMF}_j(t) + \mathrm{r}_N(t). \tag{1}$$

In new sifting, smoothing is used instead of interpolation in `Step 3c` to approximate the upper and lower envelopes of the signal (Fig. 2: box in

bold).

3. Energy separation algorithm versus Hilbert transform

Spectral estimation is the second step of EMD. This consists in demodulating IF and IA components of each IMF. An accepted way is to use Analytic Signal (AS) through HT. A crucial condition for AS to give accepted results, the signal have to be symmetric with respect to the zero mean [2]-[3]. The HT uses the whole signal (theoretically from $-\infty$ to $+\infty$). As we have a finite segment of signal the window effect will distort its spectrum. Furthermore, it is not easy to accept the use of a global operator as basis of a local estimation. An alternative way to estimate IA and IF is the DESA [8]. Based on TKEO, DESA computes these functions without involving integral transforms as in HT; it is totally based on differentiation. A distinct advantage of TKEO is its good localization. Thus, it is natural to use local operator as basis for a local estimation such as IA and IF components. Advantages of DESA are efficiency, low cost computational complexity and excellent time resolution (5-sample window). A disadvantage of DESA compared to HT is its sensitivity in very noisy environment. To reduce this sensitivity, a systematic approach is to use continuous-time expansions of discrete-time signals to numerically implement the required differentiation with closed formulas [9]-[11]. A common limit of HT and DESA is that they can not handle wideband signals. Thus the aim of this paper is to combine two non-linear and local approaches, ESA and EMD to track IA and IF of a multicomponent AM-FM signal. Associated with EMD, which acts as bandpass filter [4], ESA can handle wideband signals [6],[12]-[14]. Compared to Gabor filtering, EMD is a data driven approach that does not require neither the number of filters and the central filter frequencies

nor the rms bandwidth parameters [7]-[11]. Since IMFs are represented by BS functions, their smoothed derivatives are involved to compute TKEO and then in turn used in ESA. Finally, this process adds robustness to ESA.

4. ESA demodulation

TKEO is a tracking-energy operator [15] and its continuous version, Ψ, when operating on $s(t)$ is given by:

$$\Psi\left[s(t)\right] \stackrel{\Delta}{=} \left[\dot{s}(t)\right]^2 - s(t)\ddot{s}(t) \tag{2}$$

where $\dot{s}(t) = \frac{\partial s(t)}{\partial t}$. A useful and important property of Ψ operator is its behavior when applied to AM-FM signal $s(t)$, and its derivative

$$s(t) = a(t)\cos(2\pi \int_0^t f(\tau)d\tau) \tag{3}$$

The output of Ψ for such signal is given by

$$\Psi\left[s(t)\right] \approx a^2(t)\dot{\phi}^2(t), \quad \Psi\left[\dot{s}(t)\right] \approx a^2(t)\dot{\phi}^4(t) \tag{4}$$

With negligible approximation error under general realistic conditions, Eq. (4) shows that Ψ output is squared product of $a(t)$ and the instantaneous phase $\dot{\phi}(t)$. If we combine relations of Eq. (4) we obtain the ESA [8]:

$$f(t) \approx \frac{1}{2\pi}\sqrt{\frac{\Psi\left[\dot{s}(t)\right]}{\Psi\left[s(t)\right]}}, \quad \mid a(t) \mid \approx \frac{\Psi\left[s(t)\right]}{\sqrt{\Psi\left[\dot{s}(t)\right]}} \tag{5}$$

Relations of Eq. (4) are valid provided that narrowband assumption of $s(t)$ holds. By passing the continuous-time derivation in (4) to discrete differences, one obtains three versions of ESA namely DESA1a, DESA1 and DESA2 [8]. These versions of ESA generally deliver comparable performance with regards to the approximation errors for large classes of signals.

5. B-splines approach

BS play an important role in the sifting process as all extracted IMFs are linear combinations of splines. Since IMFs are represented by BS, it is natural to perform computational task such as differentiation in BS domain [9]. In this respect, BS versions of the EMD-ESA are derived [12]. The aim is to have an EMD-ESA with closed formula. Note that other approaches such as trigonometric interpolation can be used which is useful from an analytic point of view, but computationally it is much more expensive than BS [16]. In the present work both exact and smoothed splines are investigated. It is important to keep in mind that the definition of IMF does not specify what is required of the upper and lower envelopes, only that they pass through the maxima and minima of the signal respectively. Our approach can be easily extended to incorporate other types of splines and particularly in the sifting process. The main idea is that IMFs can be represented by any spline or other functions provided that these functions have some attractive properties such as continuity, continuity of derivatives, smoothness, simple analytical form and simple representation.

5.0.1. Demodulation by exact splines

An IMF can be written in terms of BS expansions as follows [2],[5]:

$$\mathrm{IMF}_j^n(t) = \sum_{k\in\mathbb{Z}} c_j\,[k]\,\beta_k^n(t-k) \tag{6}$$

where $\beta_k^n(t)$ and $c_j\,[k]$ are the Schoenberg's central BS of order n [17] and the BS coefficients of the jth mode, respectively. Thus IMFs derivatives can be calculated by applying finite differences to BS coefficients of the representation. For sake of clarity $\mathrm{IMF}_j^n(t)$ is replaced by $g_j^n(t)$ and then

output of TKEO for $g_j^n(t)$ and $\nabla g_j^n(t)$ are given by:

$$\begin{aligned}\Psi\left[g_j^n(t)\right] &= \left[\frac{\partial g_j^n(t)}{\partial t}\right]^2 - g_j^n(t)\frac{\partial^2 g_j^n(t)}{\partial t^2} \\ \Psi\left[\frac{\partial g_j^n(t)}{\partial t}\right] &= \left[\frac{\partial^2 g_j^n(t)}{\partial t^2}\right]^2 - \frac{\partial g_j^n(t)}{\partial t}\frac{\partial^3 g_j^n(t)}{\partial t^3}\end{aligned} \tag{7}$$

IF, $f_j(t)$, and IA, $a_j(t)$, of the jth IMF are written as follows [19]:

$$a_j(t) = \frac{\Psi\left[g_j^n(t)\right]}{\sqrt{\Psi\left[\nabla g_j^n(t)\right]}}, \quad f_j(t) = \frac{1}{2\pi}\sqrt{\frac{\Psi\left[\nabla g_j^n(t)\right]}{\Psi\left[g_j^n(t)\right]}} \tag{8}$$

where $\nabla(.) \equiv \frac{\partial(.)}{\partial t}$. To formulate ESA-BS, first derivatives of IMF are calculated. An interesting feature of BS forms is given by equation (6). Using this equation, closed-form expressions for the derivatives involving only the coefficients $c_j[n]$ and the BS function are derived:

$$\begin{aligned}\frac{\partial g_j^n(t)}{\partial t} &= \sum_{n\in\mathbb{Z}}(c_j[n] - c_j[n-1])\beta_j^{n-1}(t-n+\frac{1}{2}) \\ \frac{\partial^2 g_j^n(t)}{\partial t^2} &= \sum_{n\in\mathbb{Z}}(c_j[n+1] - 2c_j[n] + c_j[n-1])\beta_j^{n-2}(t-n) \\ \frac{\partial^3 g_j^n(t)}{\partial t^3} &= \sum_{n\in\mathbb{Z}}(c_j[n+1] - 3c_j[n] + 3c_j[n-1] - c_j[n-2]).\beta_j^{n-3}(t-n+\frac{1}{2})\end{aligned}$$

Using these derivatives in continuous ESA (Eq. 5), a closed form of EMD-ESA-BS is derived. In this work each signal $s(t)$ (IMF) is approximated by a BS of third order, $s(t) = c_1t^3 + c_2t^2 + c_3t + c_4$. Thus the closed form expressions of EMD-ESA-BS are given by

$$a_j(t) = \frac{A(t)+B(t)}{\sqrt{C(t)}}, \quad f_j(t) = \frac{1}{2\pi}\sqrt{\frac{C(t)}{A(t)+B(t)}} \tag{9}$$

where $A(t)$, $B(t)$ and $C(t)$ are given by

$$A(t) = 3c_1^2t^4 + 4c_1c_2t^3 + 2c_2^2t^2, \;\; B(t) = (2c_2c_3 - 6c_1c_4)t + c_3^2 - 2c_2c_4$$

$$C(t) \quad = \quad 18c_1^2t^2 + 12c_1c_2t + 4c_2^2t - 6c_1c_3$$

With exact splines, interpolating polynomial pass exactly through signal samples. For very noisy data, one have to use BS functions passing closely but not exactly through the signal samples using smooth BS [18].

5.0.2. Demodulation by smoothed splines

Since the sifting is an iterative process, any approximation error will propagate through all the process (Fig. 2). This is why we carefully handle the interpolation step and propose a new sifting process. More specifically, we use smoothing instead of interpolation by exact splines to construct the upper and lower envelopes. As a consequence, the number of insignificant IMFs is reduced. Indeed, key importance of the EMD is obtaining estimates of the IMFs of the sifted signal in a robust way. For noisy signals, errors in interpolating extrema (extrema due to noise) can tend to increase the amount of sifting iterations which ultimately over-decomposes the signal by spreading out their components over adjacent modes. Consequently, the number of unwanted IMFs increases. Instead, to reduce the number unwanted modes we seek a solution that is close to the data but has some inherent smoothness to counterbalance the effect of the noise. This why, smoothing is preferred to interpolation where BS envelopes pass closely but not exactly through the signal samples. To improve the performance of EMD-ESA-BS in noisy environment, an approproximate representation (smoothed splines) is more robust to noise than exact one [9]. This is done by relaxing the interpolation constraint and to find a function (solution) of order $n = 2r - 1$ that minimizes E (Eq. 10).

$$E = \sum_{l=-\infty}^{\infty} (\mathrm{IMF}_j^n(n) - h_j^n(l))^2 + \lambda \int \left(\frac{\partial^r h_j^n(t)}{\partial t^r} \right)^2 dt \qquad (10)$$

Equation (10) is well-posed regularized least-squares problem where the first term measures the error between the model $h_j^n(l)$ and the measured data $\mathrm{IMF}_j^n(n)$. The second term imposes a smoothness constraint on the solution $h_j^n(l)$. The regularization factor, λ, measures how smooth the interpolating function will be and how close to the data samples the interpolant will pass. For $\lambda = 0$ there is no smoothing and the interpolation curve fits exactly the signal samples. If $\lambda \neq 0$, the deviation to the data samples increases with the value of λ. Once the smooth BS function of each IMF is calculated, the next step is to integrate it to ESA following the same steps as for EMD-ESA-BS method. The obtained method is termed ESA Regularized BS (EMD-ESA-RBS). We illustrate in figure 1 the basic of interplolation and smoothing. Noise-free signal (marked by circles) is displayed in thin line. The noisy input is marked by stars and spline interpolant which fits the noisy input data exactly (interpolation) is represented using dotted lines. The smoothing spline is displayed in thicker line. Note that smoothing spline is comparatively much closer to noise-free signal.

6. Results and Discussion

We show the effectiveness and evaluate the performance of the new sifting (EMD-RBS) and the demodulation approach on synthetic and real signals. We first show the effect of RBS interpolation on the extracted IMFs in noisy environment. We illustrate this effect on a synthetic signal $s(t)$ with SNR=0dB:

$$s(t) = \sin(10\pi t) + n(t) \tag{11}$$

where $n(t)$ is a white Gaussian noise. Signal $s(t)$ is shown in the first row of the top diagrams of Figs. 3 and 4. In the second experiment EMD-RBS is tested on real signal derived from an hydrodynamical system. In forced

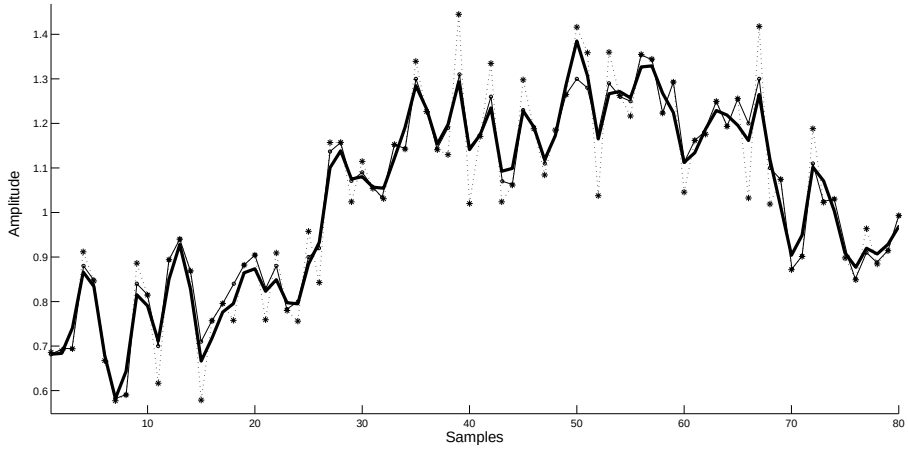

Figure 1: Interpolation vs smoothing.

oscillatory motion, one looks at the first step to separate the component of mechanical forcing (periodical oscillatory component with a known frequency) from the signal. This oscillatory component is superimposed on the original signal (top diagram of Fig. 7). This component is well identified, as IMF11, by EMD-RBS (Fig. 7) while using EMD (Fig. 6) this component is given by IMF11+IMF12 (indicated by arrows). Again, this example shows the interest of the smoothing to construct the envelopes of the signal.
In the third experiment, we study the demodulation of a signal $s(t)$ of three AM-FM components with varying noise levels:

$$s(t) = \sum_{i=1}^{3} \underbrace{(\xi_i + \kappa_i \cos(2\pi f a_i t))}_{A_i(t)} \cos(\underbrace{\pi f c_i t + \beta_i \sin(2\pi f_i t)}_{g_i(t)}) \qquad (12)$$

where κ_i and β_i are the modulation index and depth of the i^{th} signal respectively. $A_i(t)$ and $\dot{g}_i(t)$ represent the IA and the IF of i^{th} signal respectively. Parameters of $s_1(t)$, $s_2(t)$ and $s_3(t)$ are $(\xi_1 = 2.5, \kappa_1 = 0.4, fa_1 = 0.01, fc_1 = 0.25, \beta_1 = 1.8, f_1 = 0.01)$, $(\xi_2 = 0.89, \kappa_2 = 0.3, fa_2 = 0.005, fc_2 = 0.125, \beta_2 =$

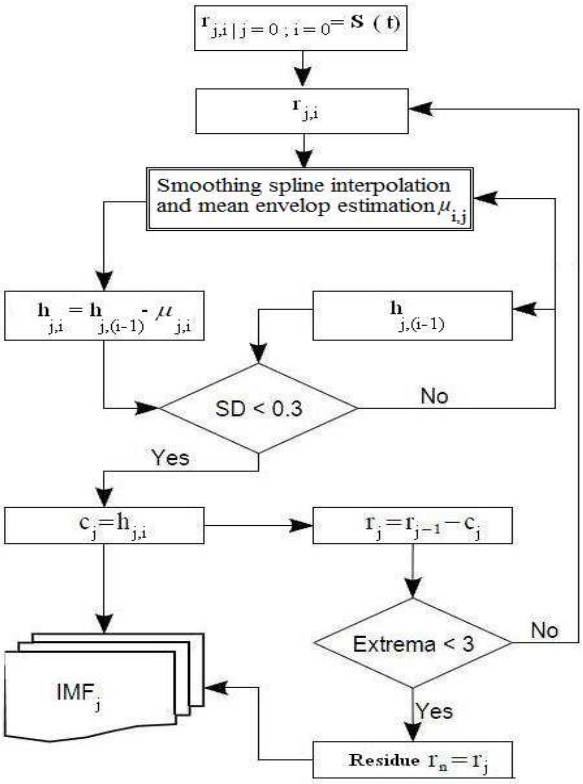

Figure 2: EMD-RBS diagram.

IA and IF estimation	EMD-DESA1	EMD-ESA-BS
IA (1^{st} component)	1.6%	1.5%
IA (2^{nd} component)	5%	5%
IA (3^{rd} component)	4%	3%
IF (1^{st} component)	22×10^{-4}	3×10^{-4}
IF (2^{nd} component)	10×10^{-5}	7×10^{-5}
IF (3^{rd} component)	7×10^{-3}	5×10^{-3}

Table 1: MSE in estimation of IF and IA of three AM-FM components signal

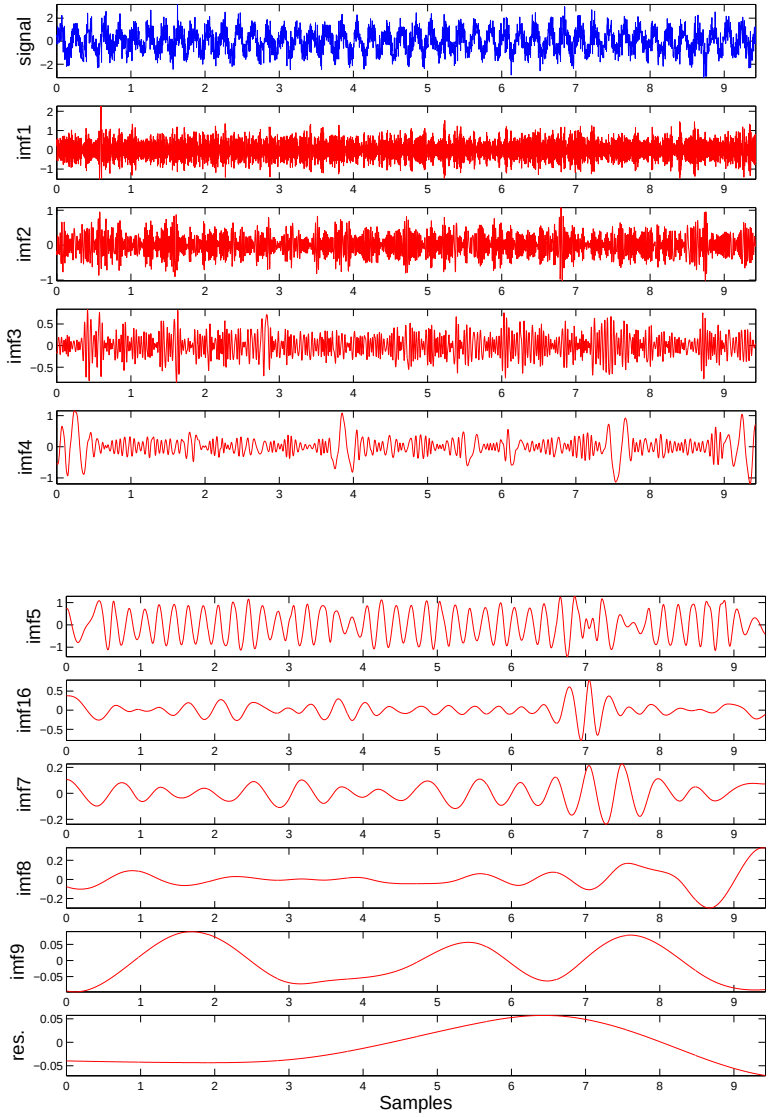

Figure 3: Decomposition of noisy signal $s(t)$ (Eq. 11) with EMD-BS (SNR=0dB)

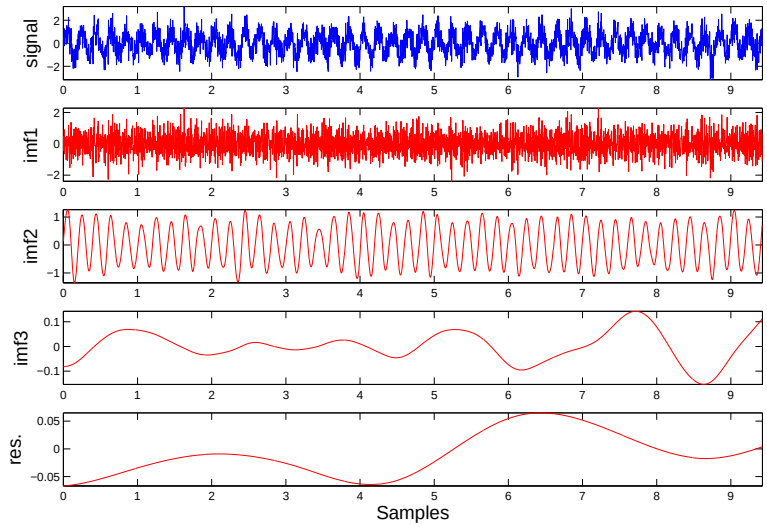

Figure 4: Decomposition of noisy signal $s(t)$ (Eq. 11) with EMD-RSB (SNR=0dB)

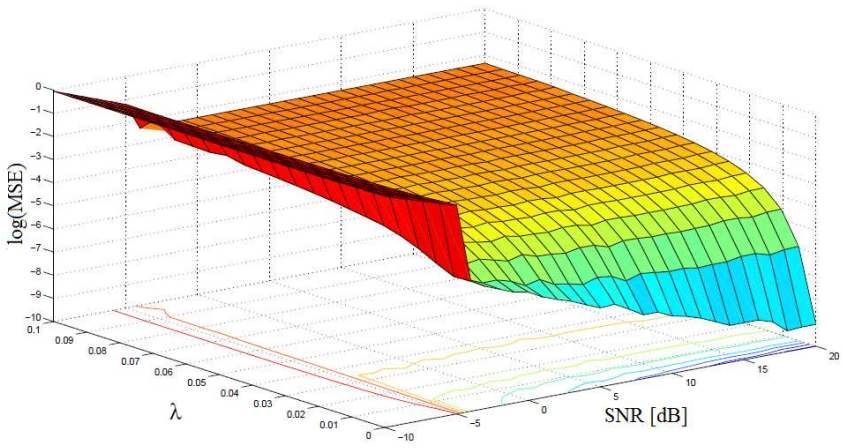

Figure 5: Variation of the λ parameter

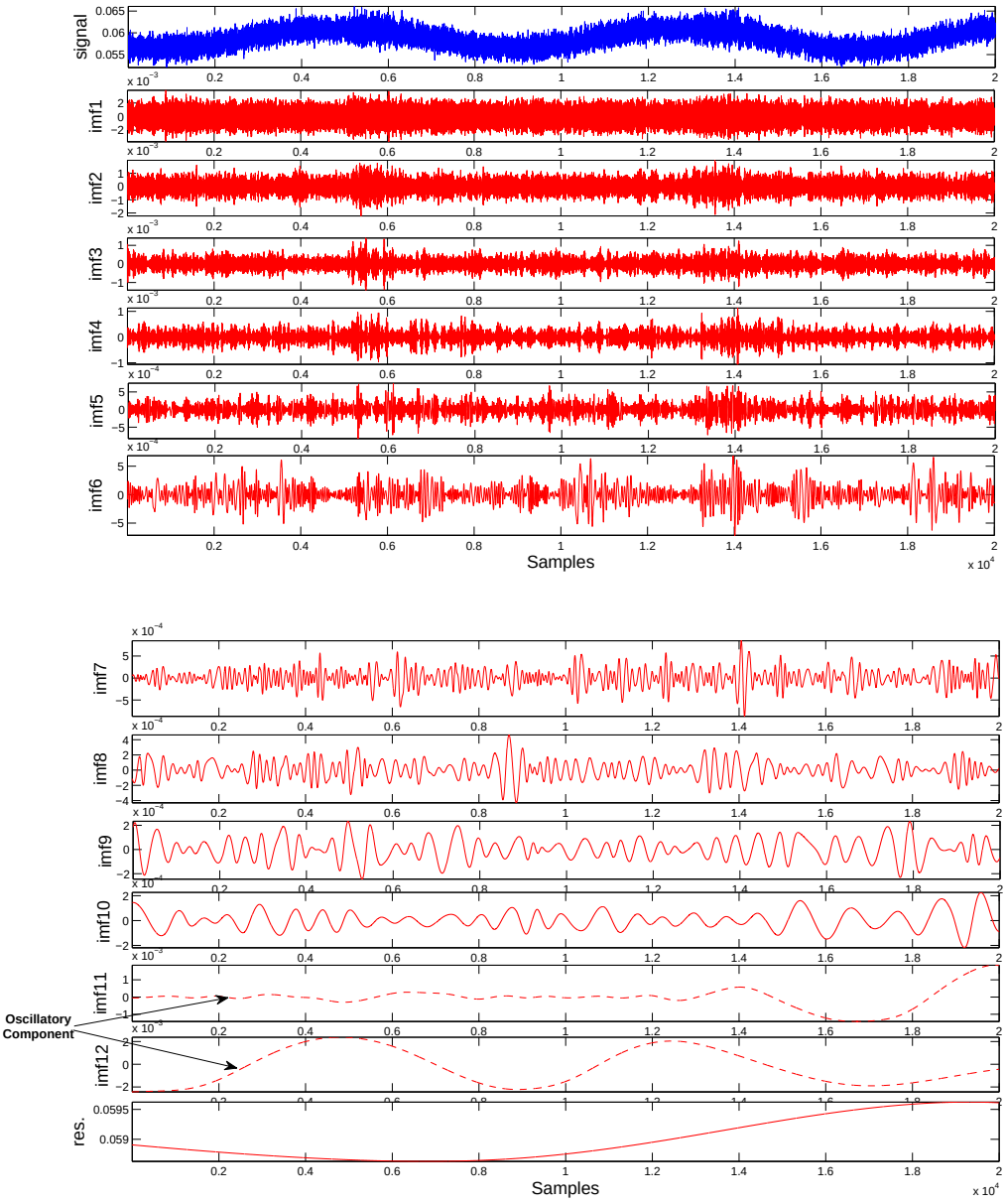

Figure 6: Extracted IMFs by EMD-BS from hydrodynamical measured signal (on top).

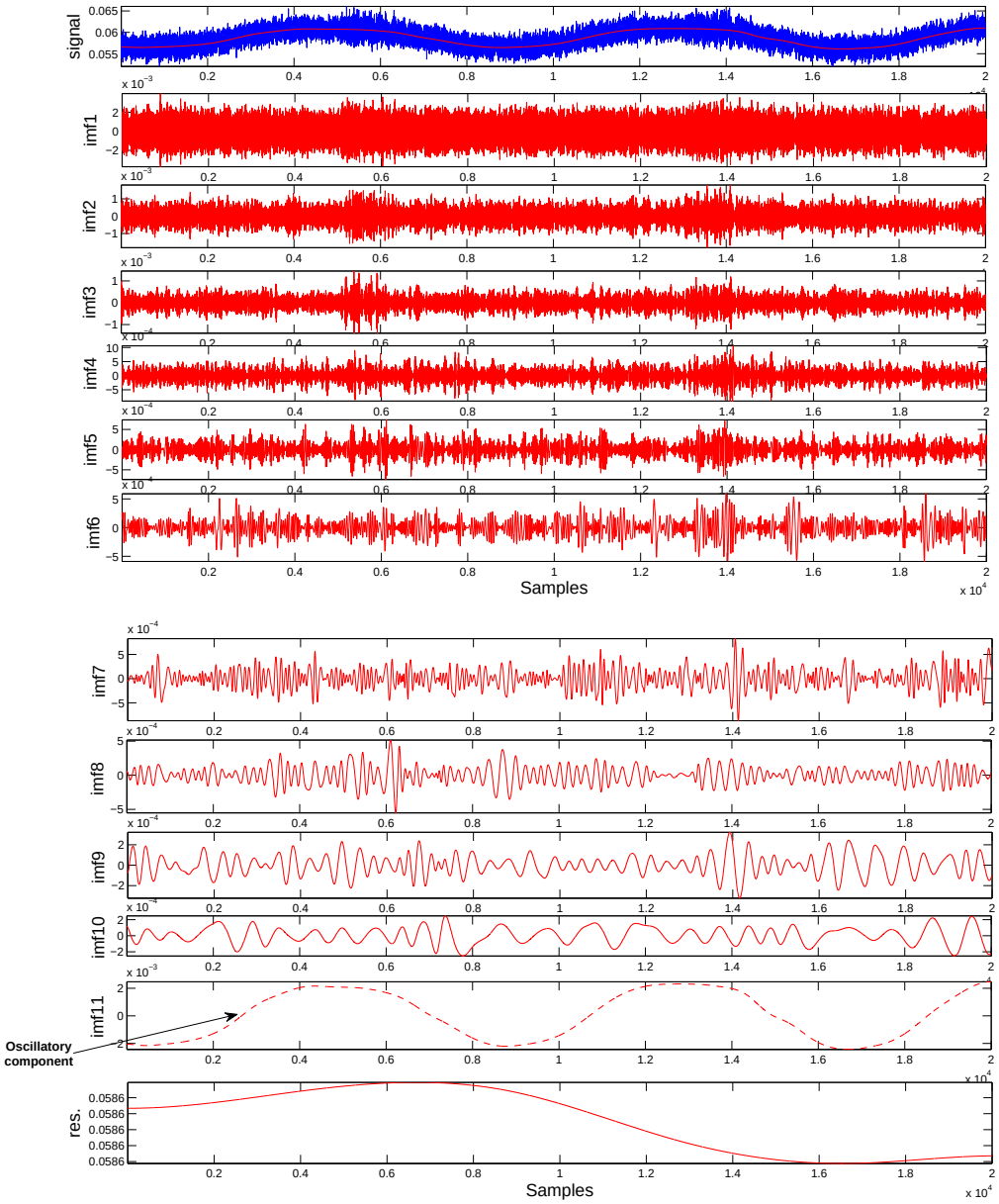

Figure 7: Extracted IMFs by EMD-RBS from hydrodynamical measured signal (on top).

$0.9, f_2 = 0.005$) and ($\xi_3 = -0.5, \kappa_3 = 0.1, fa_3 = 0.02, fc_3 = 0.0625, \beta_3 = 0.45, f_3 = 0.02$) respectively. Accuracy of EMD-ESA-BS is first tested on noise-free signal ($n(t) = 0$). IF and IA estimates of $s(t)$ are shown in Fig. 8. This plot shows that IF estimates of EMD-ESA-BS are reasonably accurate with very small MSE values less than or equal to 7×10^{-3} (Table 1). We note also a good separation of the two first IF components by EMD-ESA-BS. For IA estimates, EMD-DESA1 and EMD-ESA-BS present similar performances. Even if the energy of the sifted $s_3(t)$ signal is underestimated by EMD, associated IA component is not far from the true one. We note also few small ripples in the estimates due essentially to mode mixing phenomenon of EMD [2]. MSE values of the estimates are reported in Table 1. These results show that EMD-ESA-BS performs better than its discrete version, EMD-DESA1. This result is confirmed by accurate separating and tracking of IF components (Fig. 8). Also, to evaluate the performance of the method, errors corresponding to the estimation of six parameters $(\xi_i, \kappa_i, fa_i, fc_i, \beta_i, f_i)$ of the AM-FM model (Eq. 12) are calculated. These parameters are obtained from the estimates IA and IF waveforms. In addition an average error per method (EMD-ESA-BS, EMD-DESA, EMD-HT) is also calculated. Estimated parameters are shown in Table 2. As we can see, EMD-ESA-BS had the lowest errors in the estimations showing the robustness of the estimated parameters compared to those of EMD-HT and EMD-DESA1. These findings show the interest of BS approach. Across all the estimates, the highest errors are observed for $\kappa_1, \kappa_2, \kappa_3$ and ξ_3 parameters using EMD-HT. Finally, we report in Table 3 a quantitative study over a range of AM and FM parameters $(\xi, \kappa, fa, fc, \beta, f)$ with error analysis of EMD-ESA-BS, EMD-DESA1 and EMD-HT methods. The AM and FM parameters estimated by EMD-ESA-BS present, on average, significantly

smaller deviations w.r.t. the true values compared to those given by EMD-DESA1 and EMD-HT approaches. The performances of EMD-ESA-BS are more pronounced for f, ξ and κ parameters.

Next, performances of EMD-ESA-RBS on signal $s(t)$ with varying input SNRs ranging from -10dB to 30dB are investigated. Only graphical results for SNR=20dB are presented. Demodulation results of five established methods, namely EMD-HT, EMD-ESA-BS, EMD-DESA1, EMD-DESA1a and EMD-DESA2 are compared. Performance of these methods are examined through MSE of IF (IA) estimates. Results of each method are superimposed to true ones. Due to the space constraints of the paper, only results of EMD-HT, EMD-ESA-BS, EMD-DESA1a and EMD-ESA-RBS are presented. These results are illustrated in figures 9-16. Overall, EMD-ESA-RBS (Fig. 12) performs better in estimating the three IF components with small deviations than the other methods (Figs. 11,15,16) and particularly compared to EMD-ESA-BS and EMD-DESA1a. Ripples seen in the first IF component yielded by EMD-ESA-BS are due to exact fitting (interpolation) while those of EMD-DESA1a are attributed to sensitivity to noise of differentiations used in TKEO. Due to very low amplitude of the third IF component none of the four methods are able to correctly this last. For IA estimates, EMD-ESA-RBS (Fig. 9) outperforms, on average, EMD-ESA-BS, EMD-HT and EMD-DESA1a (Figs. 9,13,14). As for IF estimates, similar conclusions can be drawn. As expected, due exact fitting and sensitivity of instantaneous differential operator (Eq. 5) to noise, ripples are observed on the estimates of EMD-ESA-BS (Fig. 9) and EMD-DESA1a (Fig. 14). Further, the latter presents more pronounced spikes in the estimates. Concluding, these findings show the limits of the DESA and exact BS fitting (or interpolation) in presence of noise, and emphasize the interest of smooth BS

Parameters	Theory	EMD-ESA-BS	Error	EMD-DESA1	Error	EMD-HT	Error
1^{st} component							
ξ_1	2.5	2.5	0%	2.48	0.8%	2.45	2%
κ_1	0.4	0.38	5%	0.31	22.5%	0.3	25%
fa_1	0.5%	0.5%	0%	0.47%	6%	0.48%	4%
fc_1	0.25	0.24	4%	0.24	4%	0.24	4%
β_1	1.8	1.8	0%	1.8	0%	1.8	0%
f_1	1%	1%	0%	1%	0%	1%	0%
Average error			1.5%		5.5%		5.83%
2^{nd} component							
ξ_2	0.89	0.89	0%	0.75	15.73%	0.88	1.12%
κ_2	0.3	0.3	0%	0.15	50%	0.23	23.33%
fa_2	1%	1%	0%	0.98%	2%	0.98%	2%
fc_2	0.125	0.125	0%	0.109	12.8%	0.135	8%
β_2	0.9	0.9	0%	0.9	0%	0.9	0%
f_2	0.5%	0.5%	0%	0.5%	0%	0.49%	2%
Average error			0%		13.42%		6.07%
3^{rd} component							
ξ_3	-0.5	-0.49	2%	0.27	46%	-0.18	64%
κ_3	0.1	0.08	20%	0.07	30%	0.07	30%
fa_3	2%	1.9%	5%	1.8%	10%	1.9%	5%
fc_3	6.25%	6.15%	1.6%	6.12%	2.08%	6.12%	2.08%
β_3	0.45	0.45	0%	0.45	0%	0.45	0%
f_3	2%	1.6%	20%	1.5%	25%	1.6%	20%
Average error			8.1%		18.84%		20.18%

Table 2: Evaluation of the model parameters using EMD-ESA-BS, EMD-DESA1 and EMD-HT.

Parameters							Error
$\boldsymbol{\xi}$	2.1	2.3	2.5	2.7	2.9	3	
$\xi_{\text{ESA-BS}}$	2.1	2.3	2.5	2.7	2.9	3	**0%**
ξ_{DESA1}	2.1	2.31	2.48	2.65	2.85	3.1	12%
ξ_{HT}	2.09	2.33	2.45	2.66	2.75	2.95	10%
$\boldsymbol{\kappa}$	0.1	0.3	0.4	0.6	0.8	0.9	
$\kappa_{\text{ESA-BS}}$	0.11	0.33	0.38	0.58	0.77	089	**5%**
κ_{DESA1}	0.10	0.40	0.31	0.55	0.77	0.88	11%
κ_{HT}	0.12	0.52	0.30	0.55	0.70	0.79	25%
$\boldsymbol{fa}$	0.3%	0.4%	0.5%	0.7%	0.9%	1%	
$f_{a\text{ESA-BS}}$	0.31%	0.31%	0.5%	0.65%	0.88%	0.98%	**6.2%**
$f_{a\text{DESA1}}$	0.32%	0.31%	0.47%	0.60%	0.85%	0.99%	9.3%
$f_{a\text{HT}}$	0.32%	0.31%	0.48%	0.66%	0.86%	0.93%	8.3%
$\boldsymbol{fc}$	0.2	0.23	0.25	0.27	0.29	0.3	
$f_{c\text{ESA-BS}}$	0.21	0.23	0.24	0.27	0.29	0.31	**2%**
$f_{c\text{DESA1}}$	0.24	0.23	0.25	0.27	0.28	0.29	5.1%
$f_{c\text{HT}}$	0.24	0.23	0.24	0.27	0.27	0.29	5.7%
$\boldsymbol{\beta}$	1.6	1.7	1.8	1.9	2	2.1	
$\beta_{\text{ESA-BS}}$	2.1	2.03	1.8	2.02	2.2	2	11.5%
β_{DESA1}	2.01	2.00	1.8	1.95	2.25	1.9	**11.3%**
β_{HT}	2.05	2.03	1.8	2.01	2.6	2.3	15.5%
$\boldsymbol{f}$	0.3%	0.5%	1%	1.5%	1.7%	2%	
$f_{\text{ESA-BS}}$	0.21%	0.41%	1%	1.5%	1.7%	2%	**8%**
f_{DESA1}	0.21%	0.91%	1%	1.2%	1.6%	1.9%	23.8%
f_{HT}	0.21%	0.31%	1%	1.1%	1.5%	1.8%	19.4%

Table 3: Quantitaive study over a range of AM and FM parameters using EMD-ESA-BS, EMD-DESA1 and EMD-HT.

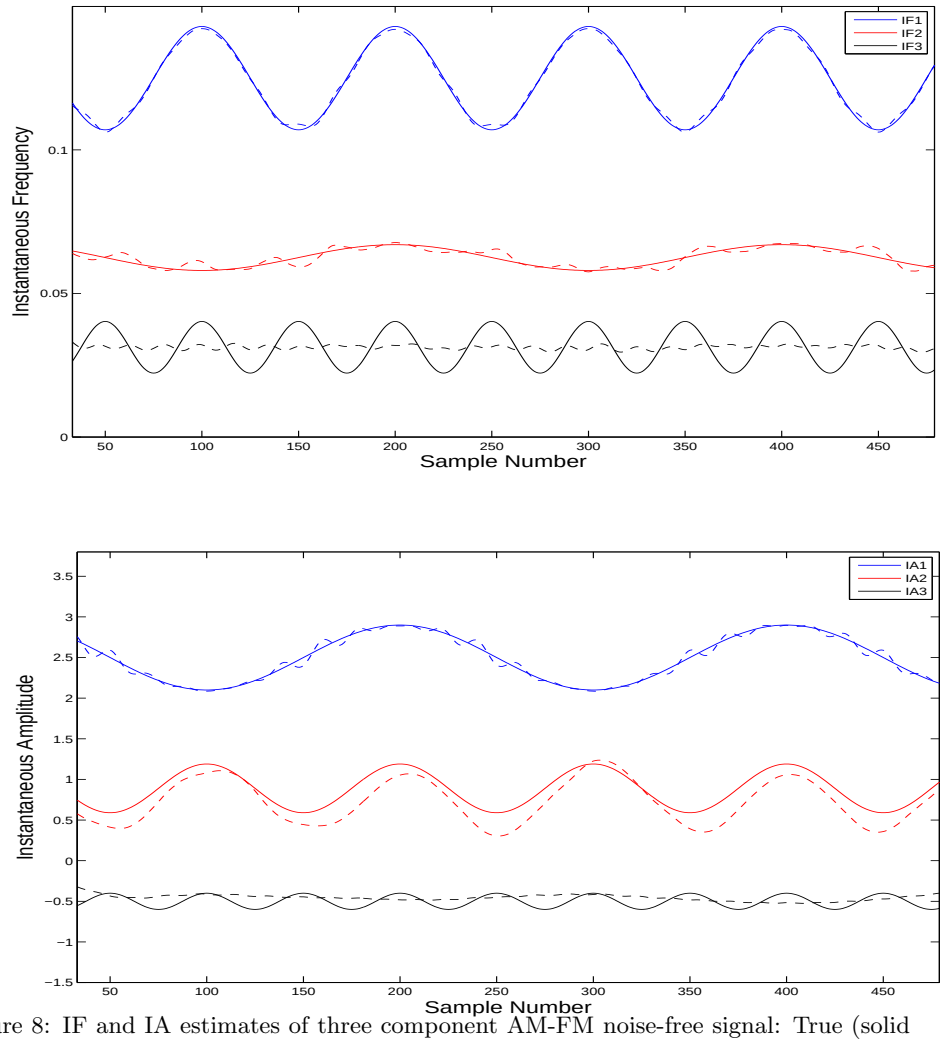

Figure 8: IF and IA estimates of three component AM-FM noise-free signal: True (solid line) and EMD-ESA-BS (dash line)

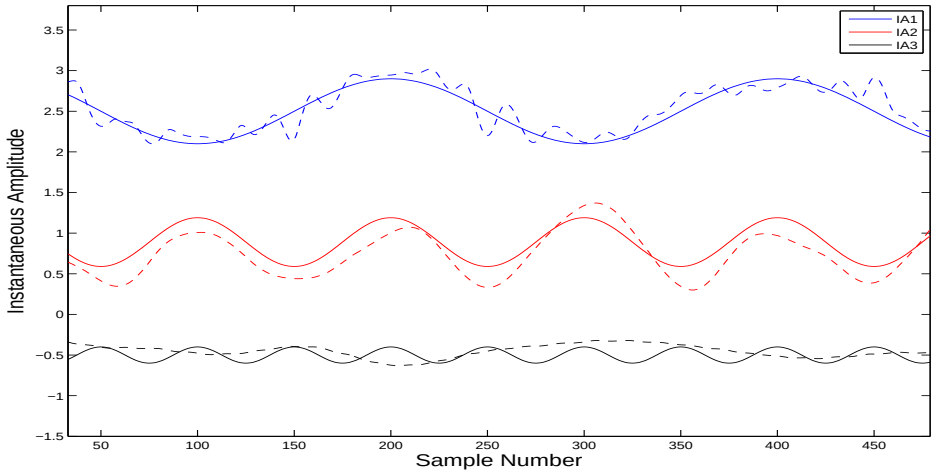

Figure 9: IA estimates of noisy multicomponent AM-FM signal: True (solid line) and EMD-ESA-BS (SNR= 20dB) (dash line)

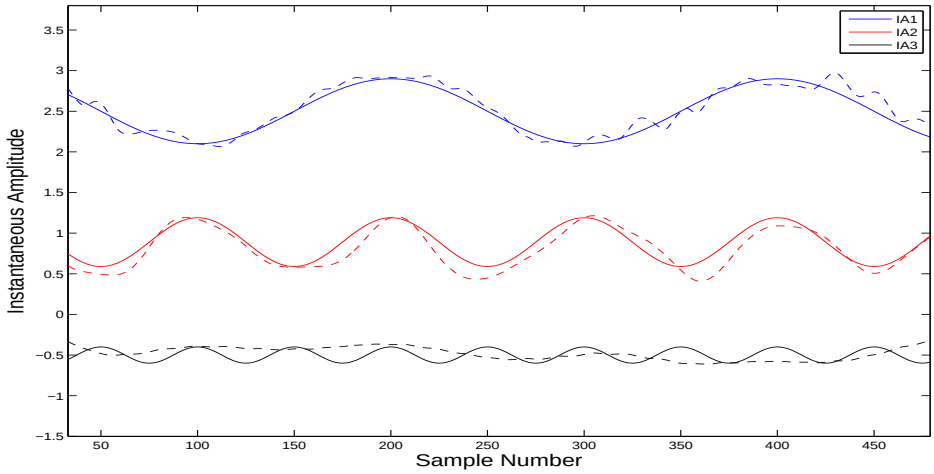

Figure 10: IA estimates of noisy multicomponent AM-FM signal: True (solid line) and EMD-ESA-RBS (SNR= 20dB) (dash line)

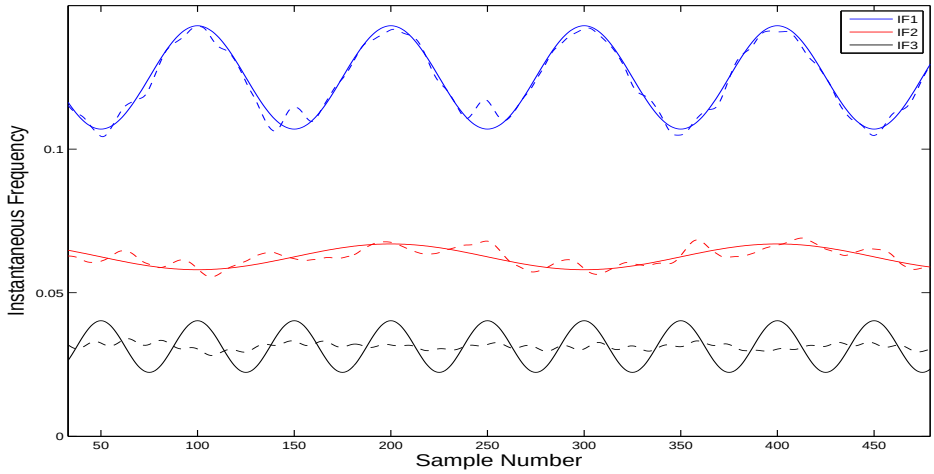

Figure 11: IF estimates of noisy multicomponent AM-FM signal: True (solid line) and EMD-ESA-BS (SNR= 20dB) (dash line)

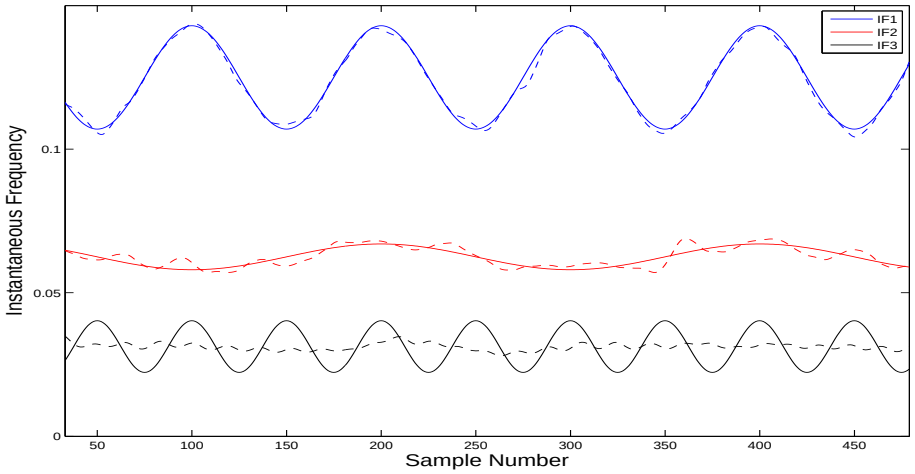

Figure 12: IF estimates of noisy multicomponent AM-FM signal: True (solid line) and EMD-ESA-RBS (SNR= 20dB) (dash line)

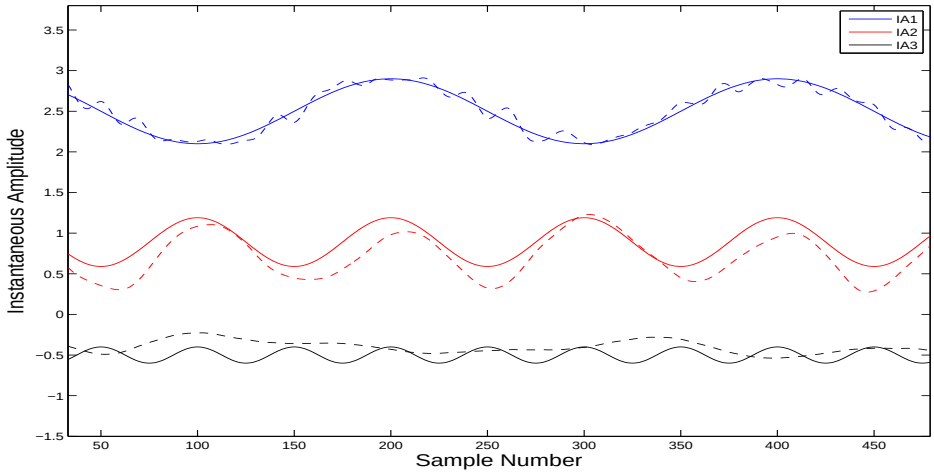

Figure 13: IA estimates of noisy multicomponent AM-FM signal: True (solid line) and EMD-HT (SNR= 20dB) (dash line)

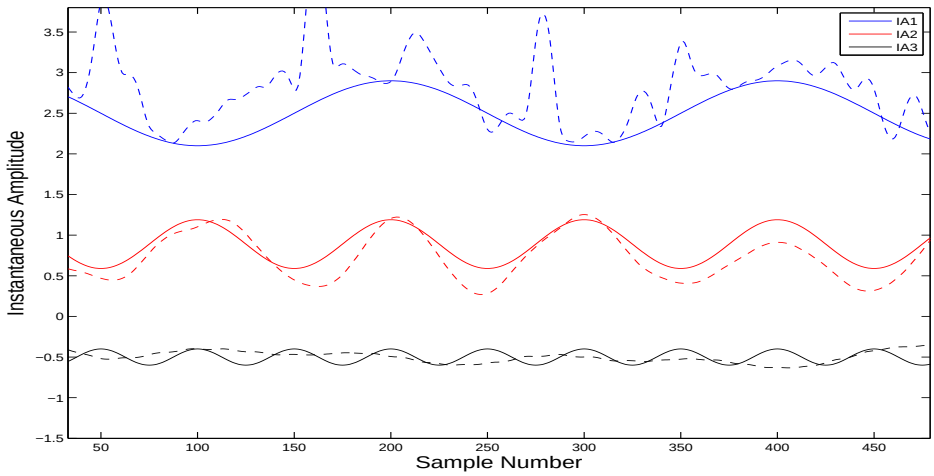

Figure 14: IA estimates of noisy multicomponent AM-FM signal: True (solid line) and EMD-DESA1a (SNR= 20dB) (dash line)

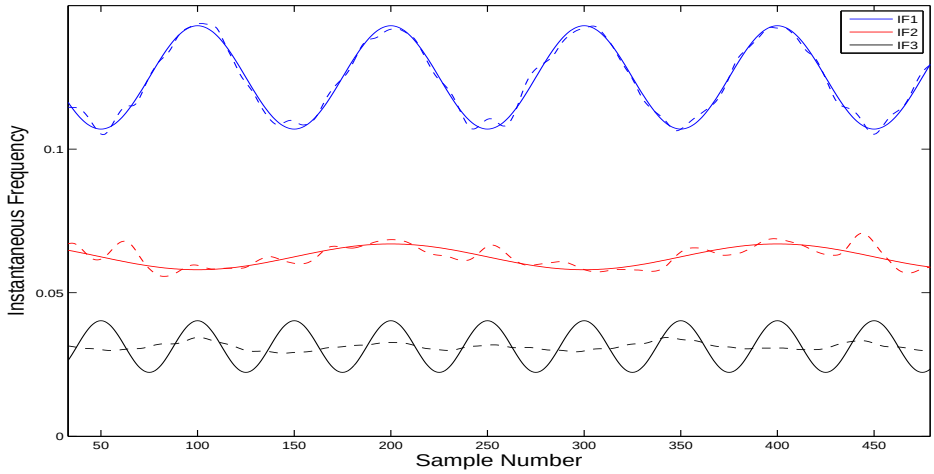

Figure 15: IF estimates of noisy multicomponent AM-FM signal: True (solid line) and EMD-HT (SNR= 20dB) (dash line)

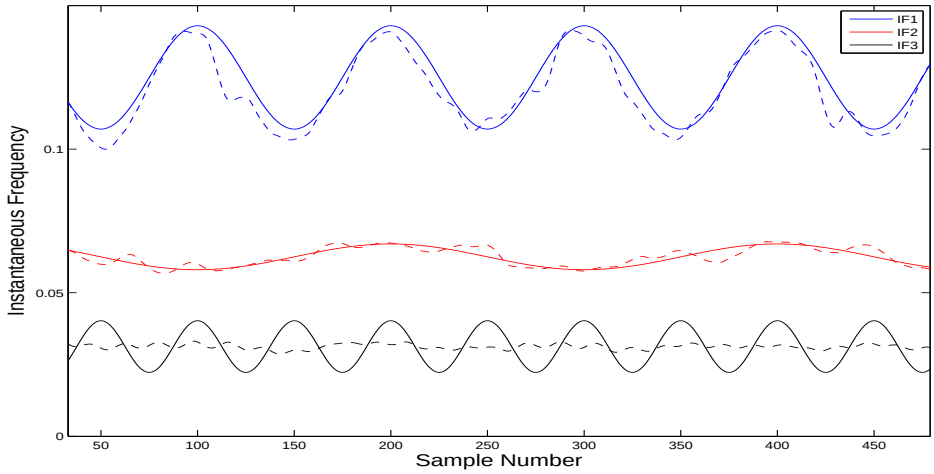

Figure 16: IF estimates of noisy multicomponent AM-FM signal: True (solid line) and EMD-DESA1a (SNR= 20dB) (dash line)

version for both ESA and EMD. Note that for both IA and IF estimates, EMD-HT (Figs. 13,15) performs better than EMD-ESA-BS (Figs. 9,11) and EMD-DESA1a (Figs. 14,16). These results are expected, since HT involves an integral transform that does implicit smoothing. Now, we compare the performance of the demodulation methods in term of MSE as function of input SNR, ranging from -7dB to 30dB, for estimation of IF component of signal $s_1(t)$. We include in this comparison EMD-DESA1 and EMD-DESA2 methods. As can be seen in the range [-7dB, 9dB] except EMD-ESA-BS the MSE of all the methods decrease (Fig. 17). Across this same range, even EMD-DESA2 and EMD-HT MSE values decrease rapidly, EMD-ESA-RBS shows significant performance improvement over the other methods. In noisy environment, signals have large variations and sharp edges and the need of smoothing factor is apparent. Thus, the performance of EMD-ESA-RBS is expected because the smooth BS gives the method more robustness in the presence of noise. In the same range, EMD-ESA-BS increases and thus performs less than EMD-ESA-RBS due essentially to exact BS fitting which increases the MSE, as the noisy samples insert a significant error. However, in moderately noisy environment, EMD-HT performs slightly better in [9dB,14dB] and this is improved in [14dB, 20dB] by EMD-BS and EMD-DESA2 methods. Toward higher SNR values ($\geq$ 16dB), the six methods display similar performances and converge, but the best result is given by ESA-based methods (Fig. 17). Note that in this range the best improvement is provided by EMD-ESA-BS because exact fitting is well suited in less noisy and noise free environments. Figure 18 compares the MSE of the six methods for IA estimates of signal $s_2(t)$. As for IF estimates of $s_1(t)$, the same tends and conclusions can be drawn. EMD-ESA-RBS performs better than the other methods in the range [-7dB, 9dB] and for higher SNR values

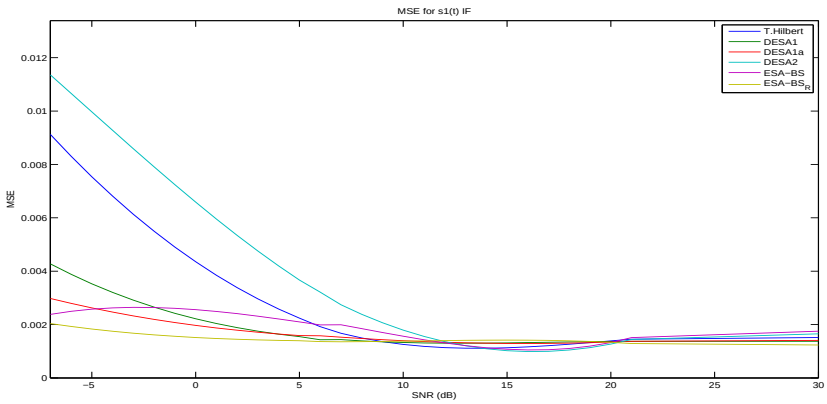

Figure 17: MSE as function of input SNR for different IF estimates for signal $s_1(t)$

($\geq$ 21dB) best results are obtained by ESA-based methods (Fig. 18). As expected EMD-ESA-BS performs less better due to the exact BS fitting in noisy conditions. Good IA estimates are given by EMD-DESA2 in [9dB, 16dB]. As in figure 17 for higher SNR values ($\geq$ 16dB), all methods perform similarly but best results are given by ESA-based methods (Fig. 18). Even from low to high SNRs (Figs. 17,18), RBS-based method shows significant performance improvement as compared to the other methods, these results are conditioned by the estimation of an optimal λ value. A careful examination of results depicted in figures 17 and 18, shows that except for low SNR values and higher ones BS-based methods do not provide the best estimates of IF and IA in moderate noise environment ([10dB, 16dB]). This again shows the difficulty to find an optimal λ value for both IA and IF estimations for all SNR ranges. Therefore, it is important to find a strategy to adapt λ to the characteristics of the analyzed signal (SNR,...).

7. Conclusion

In this work, a signal analysis framework for estimating time-varying and frequency functions of multicomponent AM-FM signals is introduced.

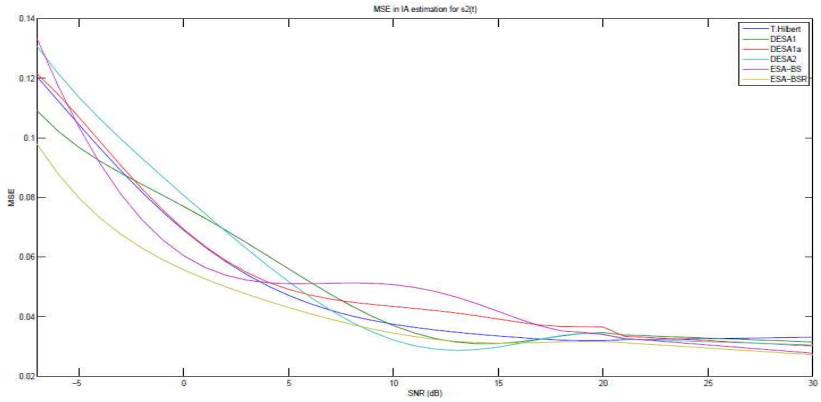

Figure 18: MSE as function of input SNR for different IA estimates for signal $s_2(t)$

The approach is based on EMD and ESA, two local approaches and not constrained by assumptions of stationarity and linearity of the signals. The proposed approach is free of cross disturbance compared for example to Wigner-Ville distribution. Furthermore, the model of narrow-band components (IMFs) and their number are not required. A new sifting process based on smoothing instead of an interpolation to construct the upper and lower envelopes of the signal is introduced. Presented results show that this sifting improves the extraction of original components from input signal and reduces the number of insignificant IMFs (over-decomposition). Consequently, analysis of extracted modes is more easier than in classical EMD showing the interest of RBS approach. Further, compared to Gabor filter bank approach which is determined by a set of parameters, EMD is data driven approach. Only SD threshold value is required. While in Gabor filtering the number of components is an input parameter (must be known), in EMD this value is automatically determined. Thus, EMD-ESA is data driven approach compared to ESA-Gabor [10]. Since extracted IMFs are represented in terms of

BS (or RBS) expansions, a closed formula of ESA is used to ensure robustness against noise compared to DESA. This new representation of a discrete signal in continuous-time domain is very important for applying ESA where signal's derivatives must be determined with high precision. Demodulation results of multicomponent AM-FM signal with varying SNRs by six well established methods are presented and compared. The results are evaluated through the MSE and estimation errors. These obtained results in free and noisy conditions show the interest of RBS approach, in term of robustness, for tracking both IA and IF functions of a multicomponent AM-FM signal. BS-based methods perform reasonably better compared to the other methods from low to high SNRs. At lower SNRs the best results are provided by EMD-ESA-RBS, showing the interest of the RBS for both EMD and ESA. The exact BS fitting is responsible in the large increase of the MSE of the demodulation method. For high SNR, on average, all the methods present similar performances but BS-based methods still perform better. Overall, the obtained results in terms of accuracy and robustness against noise, illustrate the effectiveness of the BS and RBS versions of EMD-ESA to track IF and IA features of multicomponent AM-FM signals in totally adaptive way. As all well-posed regularized least-squares problems (Eq. 10), performances of EMD-ESA-RBS are partly dependent on proper choice of λ parameter. The optimal value of λ is in general not known and is determined only through experimentation. This happens because the errors depend on the SNR, the signal and the application. As future research we plan to work on a strategy, such as L-curves, to choosing optimal λ value for both IA and IF tracking. Ongoing research work is also to apply the proposed strategy to a large class of real signals to confirm the obtained results.

References

[1] L. Cohen, *Time-frequency analysis: Theory and applications*, Prentice-Hall, 1995.

[2] N.E. Huang et *al.*, "The empirical mode decomposition and Hilbert spectrum for nonlinear and non-stationary time series analysis," *Proc. Royal Society,* vol. 454, no. 1971, pp. 903-995, 1998.

[3] N.E. Huang et *al.*, "On instantaneous frequency," *Advances in Adaptive Data Analysis,* vol. 1, no. 2, pp. 177-229, 2009.

[4] P. Flandrin, G. Rilling and P. Goncalves, "Empirical mode decomposition as a filter bank," *IEEE SPL,* vol. 11, no. 2, pp. 112-114, 2004.

[5] Q. Chen, N. Huang, S. Riemenschnieder, Y. Xu "A B-spline approach for EMD," *Adv. Comp. Math.,* vol. 24, no. 1-4, pp. 171-195, 2006.

[6] J.C. Cexus and A.O. Boudraa, "Nonstationary signals analysis by Teager-Hunag Transform (THT)," *EUSIPCO,* 5 pages, Florence, 2006.

[7] D. Dimitriadis and P. Maragos, "An improved energy demodulation algorithm using splines," *ICASSP,* pp. 1-4, Salt Lake, USA, 2001.

[8] P. Maragos, J.F. Kaiser and T.F. Quatieri, "On amplitude and frequency demodulation using energy operators," *IEEE TSP,* vol. 41, pp. 1532-1550, 1993.

[9] M. Unser, A. Aldroubi and M. Eden, "B-Spline signal processing," *IEEE TSP,* vol. 41, pp.821-848, 1993.

[10] D. Dimitriadis and P. Maragos, "Robust energy demodulation based on continuous models with application to speech recognition," *ECSCT-EUROSPEECH,* pp. 1-4, Geneva, Switzerland, 2003.

[11] D. Dimitriadis and P. Maragos, "Continuous energy demodulation and application to speech analysis," *Speech Comm.,* vol. 48, pp. 819-937, 2006.

[12] A. Bouchikhi, A.O. Boudraa, S. Benramdane and E.H.S. Diop, "Empirical mode decomposition and some operators to estimate instantaneous frequency: A comparative study," *IEEE ISCCSP*, 4 pages, 2008, Malta.

[13] A.O. Boudraa, J.C. Cexus, F. Salzenstein, L. Guillon, "IF estimation using empirical mode decomposition and nonlinear Teager energy operator," *IEEE ISCCSP,* pp. 45-48, Hammamet, Tunisia, 2004.

[14] B. Santhanam and P. Maragos, "Demodulation of discrete multicomponent AM-FM signals using periodic algebraic separation and energy demodulation," *ICASSP,* vol. 3, pp. 2409-2412, Munich, 1997.

[15] J.F. Kaiser,"On a simple algorithm to calculate the energy of a signal," *ICASSP,* pp. 381-384, Albuquerque, NM, USA, 1990.

[16] S.D. Hwaley, Les E. Atlas and H.J. Chizek, "Some properties of empirical mode type signal decomposition algorithm," *IEEE SPL,* vol. 17, no. 1, pp. 24-27, 2010.

[17] I.J. Schoenberg, "Contribution to the problem of approximation of equidistant data by analytic functions," *Quart. Appl. Math.,* vol. 4, pp. 45-99, 1946.

[18] M. Unser, S. Horbelt and T. Blu, "Fractional derivatives, splines and tomography," *EUSIPCO,* vol. IV, pp. 2017-2020, Tampere, 2000.

[19] A. Bouchikhi et A. O. Boudraa, "IF estimation of multicomponent signal by EMD and B-spline version of TKEO," *GRETSI,* pp. 817-820, 2007, Troyes, France.